

Single Photon Near Field Emission and Revival in Quantum Dots

Sergio Tafur^{} and Michael N. Leuenberger[†]*

Models of the spontaneous emission of photons coupled to the electronic states of quantum dots are important for understanding quantum interactions in dielectric media as applied to proposed solid-state quantum computers, single photon emitters, and single photon detectors. The characteristic lifetime of photon emission is traditionally modeled in the Weisskopf-Wigner approximation. Here we model the fully quantized spontaneous emission, including near field effects, of a photon from the excited state of a quantum dot beyond the Weisskopf-Wigner approximation. We propose the use of discretized central-difference approximations to describe single photon states via single photon operators in 3+1 dimensions. We further show herein that one can shift from the traditional description of electrodynamics and quantum electrodynamics, in terms of electric and magnetic fields, to one in terms of a photonic wave function and its operators using the Dirac equation for the propagation of single photons.

The field of quantum computation (QC) and quantum information technology (QIT) has recently experienced escalated activity in the search for sources of photonic states coupled to their quantum sources [1, 2]. The observed increase in activity is in part due to the suggestion that quantum information processing based on the electron spins of quantum dots (QDs), coupled through optical modes of a micro-cavity, [1] could improve on schemes based on the energy states of trapped ions [3] and nuclear spins in chemical solution [4, 5]. Some advantages of a QC scheme based on the suggested semiconductor quantum dot arrays may include greater scalability, longer spin decoherence times, longer coherence lengths, and fast interactions mediated by photons [1]. In this contribution we present a model for describing the coupling between a single photonic state to the spin states of a quantum source (such as a QD) through optical modes present in a micro-cavity. Additional applications of this model may include the design of devices aimed at single photon emission [6], single photon detection [7, 8], quantum teleportation [9, 10], quantum computing within a quantum network [2], and quantum cryptography [11, 12, 13, 14]. This model requires a description of optical modes present in photonic crystals and dielectric micro-cavities. For example, in order to successfully describe the entanglement between photons and their quantum sources, it is imperative to achieve a resolution high enough to describe whispering gallery modes [15] available in dielectric micro-cavities such as micro-disks. This is especially important in applications that contrast classical computers, which depend on bits to store and process information, to quantum comput-

ers that depend on quantum bits (qubits).

As the name suggests, quantum binary digits are a quantum representation of the on and off state as interpreted in machines like ENIAC¹ and those in existence today. It is possible to visualize the relationship between bits and qubits by means of what is known as the Bloch sphere in terms of the on $|1\rangle$ and off states $|0\rangle$ of a bit and the state of a qubit $|\Psi\rangle$. One major advantage of quantum computers is that they do not alter the Church-Turing thesis [16] since they do not allow the computation of functions which are not theoretically computable. So far it has been shown through the discoveries of Shor and others that it is possible to develop quantum algorithms for important problems like prime factorization [17], protocols for quantum error correction (QEC), and fault-tolerant QC [18]. Other algorithms in QC, that if physically implemented could be of immediate use, include Grover's Algorithm for database searches [19] and the quantum Fourier Transform [20]. Also central to the discussion on QC and QEC is the decoherence rate of qubits. It is imperative to QC to find an implementation where qubits are well isolated from their environment [16]. Among suggested implementations for QC are Raman coupled low-energy states of trapped ions [3] and nuclear spins in chemical solution [4, 5]. Qubits based on these implementations could provide the first examples of QC up to the 5 through 10 qubits level. However, these implementations may not be scalable to more than 100 qubits [1].

Proposed implementations and promising schemes that could be scalable to more than 100 coupled qubits may be based on electron spins coupled by means of an optical mode of a photonic crystal or dielectric micro-cavity. One such scheme couples the electronic spin states of a Quantum Dot (QD) to the optical modes of a micro-disk [1]. Another promising scheme couples electronic QD states embedded inside nanocavities to the modes of a photonic crystal host [21, 22, 23]. An additional scheme recently realized experimentally has shown that Nitrogen-Vacancy centers in diamond can also be embedded inside a photonic crystal, which could enable fully scalable room-temperature quantum computing as a good alternative to using quantum dots. [24, 25, 26, 27].

The discussion for generating a theory on the interaction between such quantum sources and photonic states may be modeled after atomic systems [28]. For the case of a quantum source modeled after an effective two-level QD, the selection rules presented in figure (1) yield an interaction via the dipole approximation by implementing the state to state tran-

^{*}Nanoscience Technology Center, Department of Physics, and Institute for Simulation and Training at the University of Central Florida, e-mail: stafur@mail.ucf.edu

[†]Nanoscience Technology Center and Department of Physics at the University of Central Florida, e-mail: mleuenbe@mail.ucf.edu, corresponding author

¹ Electronic Numerical Integrator And Computer

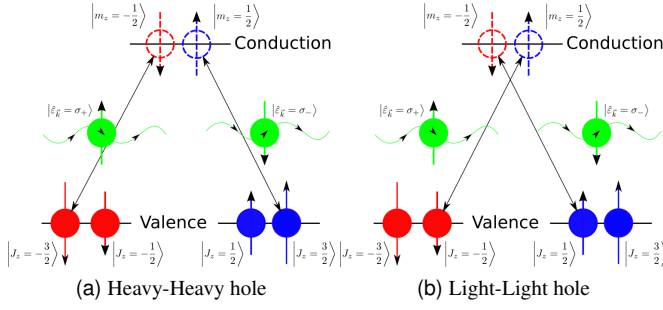


Fig. 1: Selection rules in a two-level quantum source coupling to single photon states

sition dipole moments of the QD [2]. To this end it is imperative to model spontaneous emission of a photon coupled to the electronic state of a quantum dot beyond the Weisskopf-Wigner approximation; which fixes the value of accessible modes from a possibly infinite set of frequencies ν_k to a single mode of a cavity or the transition frequency of the QD state as represented by ω_γ [28].

Our proposed model describes the photon by means of a Dirac-like equation for the photon. Experimentally, the quantum state of a photon may be reconstructed using optical homodyne tomography techniques by measuring quantum noise statistics of field amplitudes at different optical phases [29, 30]. In this work, the rigorous description of the interaction between a quantum source and the generated Maxwell Field is initially made within the formalism of relativistic quantum field theory (QFT). In this description we begin within the canonical quantization procedure presented by the Gupta and Beuler method and the resulting interaction between these fields [31]. This procedure requires the definition of a Lagrangian and gauge for the interacting fields². To follow this procedure, a connection between the photon wave function (PWF) [32, 33, 34, 35] and the four vector potential for a Maxwell Field has to be drawn. This canonical quantization procedure leads to two important results, the complex Maxwell Field Tensor and the coupled electron-photon field equations in terms of a field equation for the PWF. We show the first result to be a Lagrangian for a free complex Maxwell Field written in terms of a self-dual tensor representing the field tensor corresponding to the PWF that directly satisfies and yields equations of motion equivalent to the generalized Maxwell equations [36, 37, 38, 35]. In the second result we show the coupling between a quantum source and the Maxwell Field it generates. We additionally extend these results to show how these can be applied to model the emission of a single photon from a dielectric micro-cavity. Throughout the relativistic treatment of these fields we will maintain the Minkowski Metric to have the signature $(+, -, -, -)$, and adopt the 4-notation consistent with $x^\mu \equiv (ct, \vec{x})$, $\eta_{\mu\nu}x^\nu = x_\mu = (ct, -\vec{x})$.

Building on the work describing the PWF formalism, while working in Gaussian units in the presence of sources, one

can define a self-dual tensor in terms of the electromagnetic field tensor [36] $\mathfrak{F}^{\mu\nu} = \partial^\mu A^\nu - \partial^\nu A^\mu$ and its dual $\mathfrak{F}_{\mu\nu}^D = \frac{1}{2}\epsilon_{\mu\nu\alpha\beta}\mathfrak{F}^{\alpha\beta}$ as $\mathfrak{G}^{\mu\nu} \equiv \mathfrak{F}^{\mu\nu} - i\mathfrak{F}_{\mu\nu}^D$ in terms of the vector potential by

$$\mathfrak{G}^{\mu\nu} = (\partial^\mu A^\nu - \partial^\nu A^\mu) - \frac{i}{2}\epsilon^{\mu\nu\alpha\beta}(\partial_\mu A_\nu - \partial_\nu A_\mu)$$

from which it is possible to define a general gauge-invariant Lagrangian for a free photon via

$$\mathcal{L}_{\text{photon}} = -\frac{1}{8}\mathfrak{G}_{\mu\nu}\mathfrak{G}^{\mu\nu}$$

The same Lagrangian expressed in terms of the well known Faraday tensor[39] reads

$$\mathcal{L}_{\text{photon}} = -\frac{1}{8}(\mathfrak{F}_{\mu\nu}\mathfrak{F}^{\mu\nu} + i(\mathfrak{F}_{\mu\nu}\mathfrak{F}_D^{\mu\nu} + \mathfrak{F}_{\mu\nu}^D\mathfrak{F}^{\mu\nu}) + \mathfrak{F}_{\mu\nu}^D\mathfrak{F}_D^{\mu\nu})$$

with the corresponding matrix representation for the self-dual tensor given by

$$\mathfrak{G}^{\mu\nu} = \begin{pmatrix} 0 & iF_x^+ & iF_y^+ & iF_z^+ \\ -iF_x^+ & 0 & -F_z^+ & F_y^+ \\ -iF_y^+ & F_z^+ & 0 & -F_x^+ \\ -iF_z^+ & -F_y^+ & F_x^+ & 0 \end{pmatrix}$$

Using \vec{E} and \vec{B} to represent electric and magnetic fields respectively [40], $\vec{F}_\mp \equiv \vec{B} \pm i\vec{E}$ [33, 32, 39]. This vector may be written in terms of the Riemann-Silberstein vector [34, 35] through the identity $\vec{F}_\pm \equiv \pm i\vec{F}_\mp = \vec{E} \pm i\vec{B}$ (given that i represents the unit pseudo-scalar [41]).

We defer to the traditional Quantum Electro-Dynamics (QED) interaction between an electron, a photon, and an additional gauge field as mitigated by $\bar{\psi}\mathcal{A}_{\text{Tot}}\psi$ where $(\mathcal{A} \equiv \gamma^\mu A_\mu)$, via $\mathcal{A}_{\text{Tot}} \equiv \mathcal{A} + \mathcal{A}_{\text{Ext}}$ and therefore express the interaction Lagrangian for a gauge field A_μ and spinor $\psi \equiv \begin{pmatrix} \varphi \\ \chi \end{pmatrix}$ similar to the the description in [42] by writing

$$\mathcal{L}_{\text{Int}} = \bar{\psi}(\not{p} - m_0c)\psi - \frac{e}{c}\bar{\psi}(\mathcal{A}_{\text{Tot}})\psi - \frac{1}{8}\mathfrak{G}_{\mu\nu}\mathfrak{G}^{\mu\nu}$$

It is worth noting that this Lagrangian leads to electromagnetic fields that satisfy the principle of superposition as required by experiment along with their conservation laws and definition of spin. This is evident because there are only expressions quadratic in the field and first order time derivatives present in the action. Explicitly in terms of the relativistic equations of motion and their Hermitian conjugates

$$\left[i\hbar\gamma^\mu\partial_\mu + \frac{e}{c}\gamma^\mu A_{\mu,\text{Tot}} + m_0c \right] \bar{\psi} = 0 \quad (1)$$

$$-\frac{e}{c}\bar{\psi}\gamma^\nu\psi + \partial_\mu\mathfrak{G}^{\mu\nu} = 0 \quad (2)$$

In the non-relativistic limit working in the radiation gauge, these EOMs yield the well known Pauli-Schrödinger equation [43]. By quantizing the 3-vector potential while defining the new operators $\vec{F}_+ = \vec{\nabla} \times \vec{A} - i\frac{1}{c}\partial_t\vec{A}$ & $\vec{F}_- = \vec{\nabla} \times \vec{A} + i\frac{1}{c}\partial_t\vec{A}$,

² In the relativistic regime we set $\vec{\nabla} \cdot \vec{A} + \frac{1}{c}\partial_t\Phi = 0$.

the EOM for the photon may be expressed as a Dirac-like equation

$$\left[\frac{i\hbar}{c} \partial_t \begin{pmatrix} 0 & I \\ -I & 0 \end{pmatrix} - \frac{\hbar}{i} \partial_k \begin{pmatrix} 0 & \sigma_k^{(3)} \\ \sigma_k^{(3)} & 0 \end{pmatrix} \right] \begin{pmatrix} \vec{F}_+ \\ \vec{F}_- \end{pmatrix} = 0 \quad (3)$$

where $\sigma_k^{(3)} = -i\varepsilon_{ijk}$ with ε_{ijk} representing the Levi-Civita permutation symbol. To define the quantized interaction term we expand the gauge field operator \vec{A} in terms of creation and annihilation operators through the use of plane waves and retain a phase factor ϕ to account for its phase freedom [35]

$$\vec{A} = \sum_{\vec{k}, \lambda} \frac{c}{\nu_k} \sqrt{\frac{\hbar \nu_k}{2V}} \left(\hat{\epsilon}_{\vec{k}, \lambda} a_{\vec{k}, \lambda} e^{-i(\nu_k t - \vec{k} \cdot \vec{x})} e^{-i\phi} + \text{H.c.} \right)$$

Making the dipole approximation to the Pauli-Schrödinger equation [43], and changing to the interaction picture leads to the expression

$$i\hbar \partial_t |\varphi\rangle = e^{i\frac{\pi}{2}} \sum_{n, m, \vec{k}, \lambda} \sqrt{\frac{\hbar \nu_k}{2V}} \left(\hat{\epsilon}_{\vec{k}, \lambda} a_{\vec{k}, \lambda} e^{-i(\nu_k t - i\vec{k} \cdot \vec{x}_0)} e^{-i\phi} + \hat{\epsilon}_{\vec{k}, \lambda}^* a_{\vec{k}, \lambda}^\dagger e^{i(\nu_k t - i\vec{k} \cdot \vec{x}_0)} e^{i\phi} \right) \cdot (\vec{\wp}_{nm} \sigma_{nm} e^{i\omega_{nm} t}) |\varphi\rangle$$

Assuming that $\nu_k = c|k|$ and making use of the identity [28] $\frac{\vec{k}}{k} \times \hat{\epsilon}_{\vec{k}, \lambda} = -\sigma i \hat{\epsilon}_{\vec{k}, \lambda}$, yields that the expression for the interaction can be written in terms of the operator \vec{F}_+

$$\vec{F}_+ = e^{-i\frac{\pi}{2}} \sum_{\vec{k}} \sqrt{\frac{2\hbar \nu_k}{V}} \left(\hat{\epsilon}_{\vec{k}, +} a_{\vec{k}, +} e^{-i(\nu_k t - \vec{k} \cdot \vec{x})} e^{-i(\phi - \frac{\pi}{2})} + \hat{\epsilon}_{\vec{k}, -}^* a_{\vec{k}, -}^\dagger e^{i(\nu_k t - \vec{k} \cdot \vec{x})} e^{i(\phi - \frac{\pi}{2})} \right)$$

by shifting the phase of the interaction $\phi \rightarrow \phi - \frac{\pi}{2}$, such that at \vec{x}_0 ,

$$i\hbar \partial_t |\varphi\rangle = -\frac{1}{2} \sum_{n, m} (\vec{F}_+ - \vec{F}_-) \cdot (\vec{\wp}_{nm} \sigma_{nm} e^{i\omega_{nm} t}) |\varphi\rangle \quad (4)$$

The EOMs as derived from (4) (in terms of the photonic wave functions), for the case of a two level quantum source with an energy band-gap of $\Delta E = \hbar \omega_\sigma$, defined by the state-vector³ $|\sigma\gamma\rangle = c_a(t)|a0\rangle + c_{b,\vec{k}}(t)|b1_{\vec{k}}\rangle$ interacting with it's own spontaneously emitted field, are given by⁴

$$i\hbar \dot{c}_a(t) = \left(\vec{\Psi}_{\gamma,+}^{(+)} + \vec{\Psi}_{\gamma,-}^{*(+)} \right)_b e^{i\omega_\sigma t} \cdot \vec{\wp}_{ba}$$

$$i\hbar \sum_{\vec{k}, \pm} \dot{c}_{b,\vec{k}, \pm}(t) = \left(\vec{\Psi}_{\gamma,+}^{(-)} + \vec{\Psi}_{\gamma,-}^{*(-)} \right)_a e^{-i\omega_\sigma t} \cdot \vec{\wp}_{ab}$$

³ Where σ, γ denote electronic and photonic states and a, b denote excited and ground states

⁴ e.g. $\vec{\Psi}_{\gamma,+}^{(+)} = e^{i\frac{\pi}{2}} \sum_{\vec{k}} \sqrt{\frac{\hbar \nu_k}{2V}} c_{b,\vec{k},+}(t) \hat{\epsilon}_{\vec{k},+} e^{-i\nu_k t} e^{i\vec{k} \cdot \vec{x}_0} e^{-i(\phi - \frac{\pi}{2})}$
& $\vec{\Psi}_{\gamma,-}^{(+)} = e^{i\frac{\pi}{2}} \sum_{\vec{k}} \sqrt{\frac{\hbar \nu_k}{2V}} c_{b,\vec{k},-}(t) \hat{\epsilon}_{\vec{k},-} e^{-i\nu_k t} e^{i\vec{k} \cdot \vec{x}_0} e^{-i(\phi - \frac{\pi}{2})}$

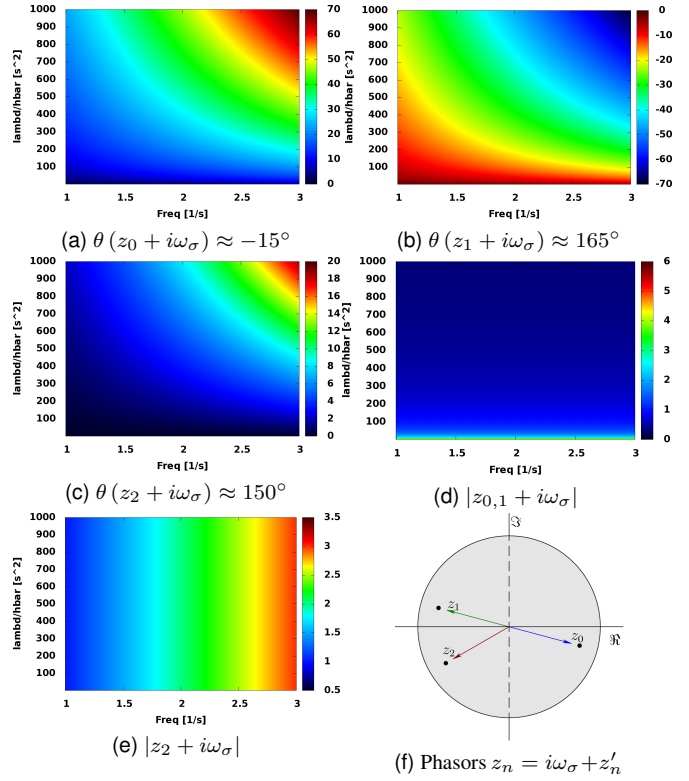


Fig. 2: Analytically evaluated poles z_n through use of Demoivre's theorem.

Plots present the relative change of the argument θ in arc-seconds $\Delta\theta''$ for z_0 & z_1 . For z_2 the change in the argument is of the order $\Delta\theta'' \times 10^{-2}$. Radial length phasors $z_n + i\omega_\sigma$ for z_0 and z_1 are of the order of $10^{19} \frac{1}{s}$ and for z_2 these are of the order of $10^{15} \frac{1}{s}$ as plotted with respect to transition frequency ω_σ in $10^{15} \frac{1}{s}$ and $\frac{\lambda}{h} = \frac{1}{4\pi} \frac{1}{3\hbar c^3} [2\vec{\wp}_{ab,x}^2 + 2\vec{\wp}_{ab,y}^2 + \vec{\wp}_{ab,z}^2]$ in $10^{-40} s^2$. Phasors with negative real components correspond to emission and those with positive real components correspond to revival in near field regions.

Formally integrating these equations of motion while representing the polarization vectors as $\hat{\epsilon}_{\vec{k},+} = \frac{1}{\sqrt{2}} (\hat{\theta} + i\hat{\phi})$, $\hat{\epsilon}_{\vec{k},-} = \frac{1}{\sqrt{2}} (\hat{\theta} - i\hat{\phi})$, and the unit wave-vector as $\hat{k} \equiv \hat{r}$, yield three poles z_n which need to be considered when solving for the probability density that ultimately gives rise to the spontaneously emitted photon, $c_{b,\vec{k},\lambda}(t)$. Each of these poles correspond to emission and re-absorption respectively and allow one to model Rabi oscillations associated with revival phenomena. These poles can be evaluated numerically or analytically by application of Demoivre's theorem.

In figure (2) we present solutions for poles z_n in for transition wavelengths and transition dipole moments in the ranges of 750 - 1300 nm and 20 to 100 Debye [44, 45, 46]. From these results, the poles of the contour integrals associated with the evaluation of $c_a(t)$ are presented as in figure (2) and their physical meaning interpreted from their location in the complex plane; where the contours are closed with further causal constraints. The expression for the wave-function, prior to its

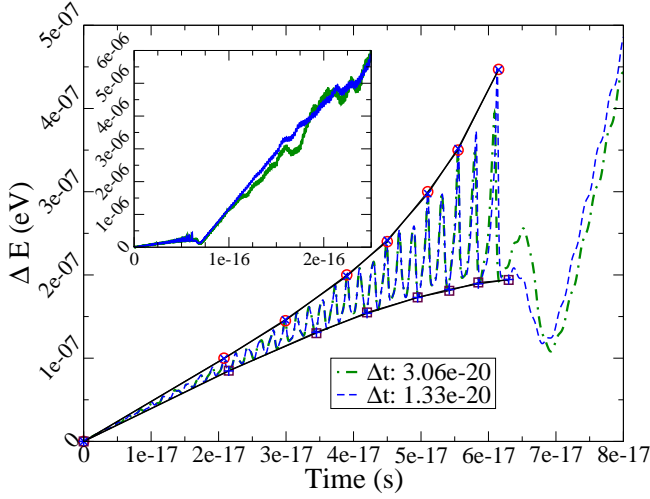


Fig. 3: Near field revival phenomena represented in terms of energy exchange ΔE (eV) between the QD state and the single photon for coarse and fine time steps. Envelope functions bounding the region of coherent oscillation behave as low order polynomials. The polynomial behavior of the envelope functions is contradictory to the expectation of exponential behavior with characteristic times of the order of the roots z_n for c_a .

propagation through (3) is

$$\vec{\Psi}_{\gamma,-,b}^{*(+)}(t) = \frac{-1}{(2\pi)^3} \sum_{n=1}^3 A_n \vec{I}_{-,n} + \vec{\Psi}_{\gamma,-,b}^{*(+)}(t_0) \quad (5)$$

$$\vec{\Psi}_{\gamma,+,b}^{(+)}(t) = \frac{-1}{(2\pi)^3} \sum_{n=1}^3 A_n \vec{I}_{+,n} + \vec{\Psi}_{\gamma,+,b}^{(+)}(t_0) \quad (6)$$

In this result we do not neglect terms of order $O\{r^{-2}\}$, usually neglected in the far-field approximation [28]. Writing $\vec{\varphi}_{ab,i} \rightarrow \vec{\varphi}_i$ along with $\Omega_n = \omega_\sigma + iz_n$ and $\mathbf{z} = \vec{x} - \vec{x}_0$, and setting the speed of light within the interaction region to $c_0 = \eta^{-1}c$, the components for an “emitting” pole with the contour closed over the lower half plane, are given by

$$\mathcal{I}_{\pm,n,z} = \left[\left(\frac{1}{\mathbf{z}^3} - \frac{i\Omega_n}{\mathbf{z}^2 c_0} \right) \zeta_- - \left(\frac{1}{\mathbf{z}^3} + \frac{i\Omega_n}{\mathbf{z}^2 c_0} \right) \zeta_+ \right] \vec{\varphi}_z$$

$$\begin{aligned} \mathcal{I}_{\pm,n,x} = & \left[\left(\pm i\vec{\varphi}_y + \frac{(1 \pm 1)}{2} \vec{\varphi}_x \right) \frac{\Omega_n^2}{\mathbf{z} c_0^2} + (\vec{\varphi}_x \pm \vec{\varphi}_y) \frac{i\Omega_n}{\mathbf{z}^2 c_0} - \frac{\vec{\varphi}_x}{\mathbf{z}^3} \right] \frac{\zeta_-}{2} \\ & - \left[\left(\pm i\vec{\varphi}_y - \frac{(1 \pm 1)}{2} \vec{\varphi}_x \right) \frac{\Omega_n^2}{\mathbf{z} c_0^2} + (\vec{\varphi}_x \mp \vec{\varphi}_y) \frac{i\Omega_n}{\mathbf{z}^2 c_0} + \frac{\vec{\varphi}_x}{\mathbf{z}^3} \right] \frac{\zeta_+}{2} \end{aligned}$$

$$\begin{aligned} \mathcal{I}_{\pm,n,y} = & \left[\left(\mp i\vec{\varphi}_x - \frac{(1 \mp 1)}{2} \vec{\varphi}_y \right) \frac{\Omega_n^2}{\mathbf{z} c_0^2} + (\vec{\varphi}_y \pm \vec{\varphi}_x) \frac{i\Omega_n}{\mathbf{z}^2 c_0} - \frac{\vec{\varphi}_y}{\mathbf{z}^3} \right] \frac{\zeta_-}{2} \\ & - \left[\left(\mp i\vec{\varphi}_x + \frac{(1 \mp 1)}{2} \vec{\varphi}_y \right) \frac{\Omega_n^2}{\mathbf{z} c_0^2} + (\vec{\varphi}_y \mp \vec{\varphi}_x) \frac{i\Omega_n}{\mathbf{z}^2 c_0} + \frac{\vec{\varphi}_y}{\mathbf{z}^3} \right] \frac{\zeta_+}{2} \end{aligned}$$

as governed by the conditions that follow from the fact that the outgoing ζ_- and incoming ζ_+ wave-fronts can not move faster than the speed of light.

$$\zeta_- = 4\pi^2 \Theta(c_0 \Delta t' - \mathbf{z}) e^{-i\Omega_n(\Delta t' - \frac{\mathbf{z}}{c_0} + t_0)}$$

$$\zeta_+ = 4\pi^2 \Theta(c_0 \Delta t' + \mathbf{z}) e^{-i\Omega_n(\Delta t' + \frac{\mathbf{z}}{c_0} + t_f)}$$

We additionally go beyond the approximations which neglect revival [28], such that the components of an “absorbing” pole with the contour closed over the upper half plane, are given by

$$\mathcal{I}_{\pm,n,z} = \left[\left(\frac{1}{\mathbf{z}^3} - \frac{i\Omega_n}{\mathbf{z}^2 c_0} \right) \zeta_- - \left(\frac{1}{\mathbf{z}^3} + \frac{i\Omega_n}{\mathbf{z}^2 c_0} \right) \zeta_+ \right] \vec{\varphi}_z$$

$$\mathcal{I}_{\pm,n,x} =$$

$$\begin{aligned} & \left[\left(\pm i\vec{\varphi}_y - \frac{(1 \pm 1)}{2} \vec{\varphi}_x \right) \frac{\Omega_n^2}{\mathbf{z} c_0^2} + (\vec{\varphi}_x \mp \vec{\varphi}_y) \frac{i\Omega_n}{\mathbf{z}^2 c_0} + \frac{\vec{\varphi}_x}{\mathbf{z}^3} \right] \frac{\zeta_+}{2} \\ & - \left[\left(\mp i\vec{\varphi}_y - \frac{(1 \pm 1)}{2} \vec{\varphi}_x \right) \frac{\Omega_n^2}{\mathbf{z} c_0^2} - (\vec{\varphi}_x \pm \vec{\varphi}_y) \frac{i\Omega_n}{\mathbf{z}^2 c_0} + \frac{\vec{\varphi}_x}{\mathbf{z}^3} \right] \frac{\zeta_-}{2} \end{aligned}$$

$$\mathcal{I}_{\pm,n,y} =$$

$$\begin{aligned} & \left[\left(\mp i\vec{\varphi}_x + \frac{(1 \mp 1)}{2} \vec{\varphi}_y \right) \frac{\Omega_n^2}{\mathbf{z} c_0^2} + (\vec{\varphi}_y \mp \vec{\varphi}_x) \frac{i\Omega_n}{\mathbf{z}^2 c_0} - \frac{\vec{\varphi}_y}{\mathbf{z}^3} \right] \frac{\zeta_+}{2} \\ & - \left[\left(\pm i\vec{\varphi}_x + \frac{(1 \mp 1)}{2} \vec{\varphi}_y \right) \frac{\Omega_n^2}{\mathbf{z} c_0^2} - (\vec{\varphi}_y \pm \vec{\varphi}_x) \frac{i\Omega_n}{\mathbf{z}^2 c_0} - \frac{\vec{\varphi}_y}{\mathbf{z}^3} \right] \frac{\zeta_-}{2} \end{aligned}$$

as governed again by the conditions that follow from the fact that the outgoing ζ_- and incoming ζ_+ wave-fronts can not move faster than the speed of light

$$\zeta_- = 4\pi^2 \Theta(c_0 \Delta t' - \mathbf{z}) e^{-i\Omega_n(\Delta t' - \frac{\mathbf{z}}{c_0} + t_f)}$$

$$\zeta_+ = 4\pi^2 \Theta(c_0 \Delta t' + \mathbf{z}) e^{-i\Omega_n(\Delta t' + \frac{\mathbf{z}}{c_0} + t_0)}$$

The coupling between (3), (5), and (6) was modeled computationally through use of the following algorithm as implemented in a leap-frogging scheme [47] between real and imaginary parts of the wave-functions, both within and beyond the interaction regions.

- Initialize QD excited state
- Determine analytic approximation for c_a
- Use the leading coefficients and roots of the analytic form of c_a to determine the state of the photonic wave function $\vec{\Psi}_{\gamma,+,b}^{(+)}$ & $\vec{\Psi}_{\gamma,-,b}^{*(+)}$ at the next time step
- At this new time step use the current state of the photonic wave function to update the state of the quantum dot
- Propagate $\vec{\Psi}_{\gamma,+,b}^{(+)}$ & $\vec{\Psi}_{\gamma,-,b}^{*(+)}$
- Repeat from step 2

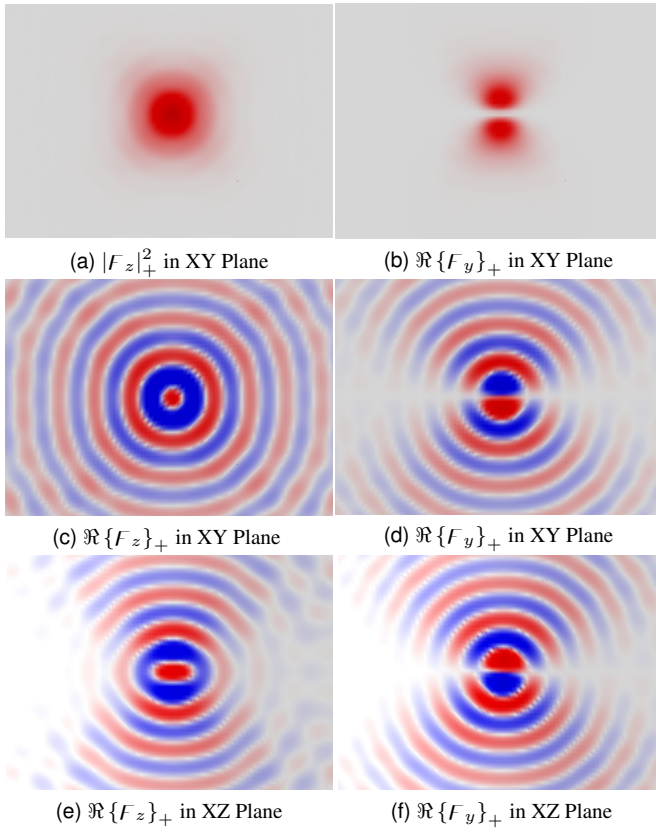


Fig. 4: Finite difference models of the spontaneous emission of a single photon from a two-level system of quantum dot states. Color intensity in red (positive) and blue (negative) represent the amplitude of the photonic wave-function field strengths.

Figure (3) shows the stable near-field exchange of energy between the quantum dot and single photon states. These results are derived from two computational experiments set to have the same ratio of $\frac{\Delta x}{\Delta t}$. It is interesting to note that the envelope functions for both of these are very similar and both exhibit a seemingly linear decay of energy shortly after an initial revival of the quantum dot state. This seems to suggest that though it is worth while to retain a time resolution small enough to observe the initial revival event, this resolution can be made coarser almost immediately following the first revival. Figure (4) presents spatial XY and XZ plane projections of single photon state components $F_{y,+}$, $F_{z,+}$ and their probability amplitudes immediately following the establishment of coherent oscillations within the polynomial envelope functions shown in Figure (3). It is evident that during this time, though evanescent modes appear to escape the quantum dot region, calculation of the localization of the single photon wave-function find the single photon state to be localized to the quantum dot region in figures (4a) & (4b). The dipolar structure in the projections presented by figures (4c) & (4e) was expected due to the initial orientation solely along the z-axis of the transition dipole moment of the two associated quantum dot levels.

We have demonstrated that it is feasible to study near field single photon emission within dielectric structures by means of the Riemann-Silberstein wave-function beyond the

Weisskopf-Wigner approximation; both analytically and computationally. It was further demonstrated that the locality of a photonic state could be well described during spontaneous emission while energy is injected and exchanged between both single photon and quantum dot states. Test cases were directly compared for different values of Δx & Δt . From these it was determined that the polynomial envelope functions for coherent oscillations were in agreement within the initial revival period of the quantum dot excited state. Furthermore, the theoretical approximations made accurately yield analytic and intuitive insight to the periodicity of the initial decay and revival phenomena present in the near field limit. This work therefore makes it feasible to computationally design photonic states to be emitted and detected by solid-state quantum dots embedded within dielectric structures and to compare them to experimental results by means of their corresponding density matrix and Wigner functions.

References

- [1] A. Imamoglu, D. D. Awschalom, G. Burkard, D. P. DiVincenzo, D. Loss, M. Sherwin, and A. Small. Quantum information processing using quantum dot spins and cavity qed. *Physical Review Letters*, 83(20), November 1999. 1
- [2] HP Seigneur, M.N. Leuenberger, and WV Schoenfeld. Single-photon Mach-Zehnder interferometer for quantum networks based on the single-photon Faraday effect. *Journal of Applied Physics*, 104:014307, 2008. 1, 2
- [3] JI Cirac and P. Zoller. Quantum computations with cold trapped ions. *Physical Review Letters*, 74(20):4091–4094, 1995. 1
- [4] D.G. Cory, A.F. Fahmy, and T.F. Havel. Ensemble quantum computing by nuclear magnetic resonance spectroscopy. *Proc. Nat. Acad. Sci.*, 94:1634–1639, 1997. 1
- [5] N.A. Gershenfeld and I.L. Chuang. Bulk spin-resonance quantum computation. *Science*, 275(5298):350, 1997. 1
- [6] Z. Yuan, B.E. Kardynal, R.M. Stevenson, A.J. Shields, C.J. Lobo, K. Cooper, N.S. Beattie, D.A. Ritchie, and M. Pepper. Electrically driven single-photon source. *Science*, 295(5552):102, 2002. 1
- [7] S. Komiyama, O. Astafiev, V. Antonov, T. Kutsuwa, and H. Hirai. A single-photon detector in the far-infrared range. *Nature*, 403(6768):405–407, 2000. 1
- [8] O. Astafiev, S. Komiyama, T. Kutsuwa, V. Antonov, Y. Kawaguchi, and K. Hirakawa. Single-photon detector in the microwave range. *Applied Physics Letters*, 80:4250, 2002. 1
- [9] D. Bouwmeester, J.W. Pan, K. Mattle, M. Eibl, H. Weinfurter, and A. Zeilinger. Experimental quantum teleportation. *Nature*, 390(6660):575–579, 1997. 1
- [10] C.H. Bennett, G. Brassard, C. Crepeau, R. Jozsa, A. Peres, and W.K. Wootters. Teleporting an unknown quantum state via dual classical and Einstein-Podolsky-Rosen channels. *Physical Review Letters*, 70(13):1895–1899, 1993. 1
- [11] C.H. Bennett, G. Brassard, et al. Quantum cryptography: Public key distribution and coin tossing. In *Proceedings of IEEE International Conference on Computers, Systems and Signal Processing*, volume 175. Bangalore, India, 1984. 1
- [12] A.K. Ekert. Quantum cryptography based on Bell’s theorem. *Physical Review Letters*, 67(6):661–663, 1991. 1
- [13] DS Naik, CG Peterson, AG White, AJ Berglund, and PG Kwiat. Entangled state quantum cryptography: eavesdropping on the Ekert protocol. *Physical Review Letters*, 84(20):4733–4736, 2000. 1
- [14] R. Ursin, F. Tiefenbacher, T. Schmitt-Manderbach, H. Weier, T. Scheidl, M. Lindenthal, B. Blauensteiner, T. Jennewein, J. Perdigues, P. Trojek, et al. Entanglement-based quantum communication over 144 km. *Nature Physics*, 3(7):481–486, 2007. 1
- [15] SL McCall, AFJ Levi, RE Slusher, SJ Pearton, and RA Logan. Whispering-gallery mode microdisk lasers. *Applied physics letters*, 60(3):289, 1992. 1
- [16] M.A. Nielsen, I. Chuang, and L.K. Grover. Quantum computation and quantum information. *American Journal of Physics*, 70:558, 2002. 1

- [17] P.W. Shor. Algorithms for quantum computation: Discrete logarithms and factoring. In *ANNUAL SYMPOSIUM ON FOUNDATIONS OF COMPUTER SCIENCE*, volume 35, pages 124–124. Citeseer, 1994. 1
- [18] P.W. Shor. Fault-tolerant quantum computation. In *Annual Symposium on Foundations of Computer Science*, volume 37, pages 56–67, 1996. 1
- [19] L.K. Grover. A fast quantum mechanical algorithm for database search. In *Proceedings of the twenty-eighth annual ACM symposium on Theory of computing*, page 219. ACM, 1996. 1
- [20] L. Hales and S. Hallgren. An improved quantum Fourier transform algorithm and applications. In *ANNUAL SYMPOSIUM ON FOUNDATIONS OF COMPUTER SCIENCE*, volume 41, pages 515–525, 2000. 1
- [21] M.N. Leuenberger, M.E. Flatté, and DD Awschalom. Teleportation of electronic many-qubit states encoded in the electron spin of quantum dots via single photons. *Physical review letters*, 94(10):107401, 2005. 1
- [22] M.N. Leuenberger. Fault-tolerant quantum computing with coded spins using the conditional Faraday rotation in quantum dots. *Physical Review B*, 73(7):75312, 2006. 1
- [23] G. Gonzalez, M.N. Leuenberger, H. Seigneur, and W.V. Schoenfeld. Theory of a Scalable Electron-Spin Based Quantum Network Inside a Photonic Crystal. *Journal of Computational and Theoretical Nanoscience*, 7(9):1651–1672, 2010. 1
- [24] D. Awschalom, R. Epstein, and R. Hanson. The diamond age of spintronics. *Scientific American Magazine*, 297(4):84–91, 2007. 1
- [25] C.F. Wang, R. Hanson, DD Awschalom, EL Hu, T. Feygelson, J. Yang, and JE Butler. Fabrication and characterization of two-dimensional photonic crystal microcavities in nanocrystalline diamond. *Applied Physics Letters*, 91:201112, 2007. 1
- [26] G. González and M.N. Leuenberger. The dynamics of the optically driven Λ transition of the 15N–V- center in diamond. *Nanotechnology*, 21:274020, 2010. 1
- [27] G. González and M.N. Leuenberger. Theory of optical Λ transitions in the $\{15\}$ NV $\{-\}$ center in diamond: Role of the hyperfine interaction. *Physical Review B*, 80(20):201201, 2009. 1
- [28] Marlan O. Scully and M. Suhail Zubairy. *Quantum Optics*. Cambridge University Press, 6 edition, 2008. 1, 2, 3, 4
- [29] U. Leonhardt. Quantum-state tomography and discrete Wigner function. *Physical review letters*, 74(21):4101–4105, 1995. 2
- [30] AI Lvovsky and MG Raymer. Continuous-variable optical quantum-state tomography. *Reviews of Modern Physics*, 81(1):299–332, 2009. 2
- [31] James D. Bjorken. *Relativistic quantum fields*. International series in pure and applied physics. McGraw-Hill, New York, 1965. 2
- [32] R. H. Good. Particle aspect of the electromagnetic field equations. *Phys. Rev.*, 105(6):1914–1919, Mar 1957. 2
- [33] H.E. Moses. Solution of Maxwell’s equations in terms of a spinor notation: the direct and inverse problem. *Physical Review*, 113(6):1670–1679, 1959. 2
- [34] I. Bialynicki-Birula. On the wave function of the photon. *Acta Physica Polonica-Series A General Physics*, 86(1):97–116, 1994. 2
- [35] B.J. Smith and MG Raymer. Photon wave functions, wave-packet quantization of light, and coherence theory. *New Journal of Physics*, 9:414, 2007. 2, 3
- [36] A. Gersten. Maxwell equations - The one-photon quantum equation. *Foundations of Physics*, 31(8):1211–1231, 2001. 2
- [37] VV Varlamov. Maxwell field on the Poincare group. *INTERNATIONAL JOURNAL OF MODERN PHYSICS A*, pages 4095–4112, JUL 10. 2
- [38] I. Bialynicki-Birula. V Photon Wave Function. *Progress in Optics*, 36:245–294, 1996. 2
- [39] L.D. Landau and E.M. Lifshitz. *The classical theory of fields*. Butterworth-Heinemann, 1980. 2
- [40] D.J. Griffiths and C. Inglefield. *Introduction to electrodynamics*. Prentice Hall New Jersey, 1999. 2
- [41] V. De Sabbata and B.K. Datta. *Geometric algebra and applications to physics*. Taylor & Francis Group, 2007. 2
- [42] K. Huang. *Quantum field theory: From operators to path integrals*. Wiley-VCH, 2010. 2
- [43] J.J. Sakurai. *Advanced quantum mechanics*. Pearson Education India, 2006. 2, 3
- [44] KL Silverman, RP Mirin, ST Cundiff, and AG Norman. Direct measurement of polarization resolved transition dipole moment in InGaAs/GaAs quantum dots. *Applied Physics Letters*, 82:4552, 2003. 3
- [45] PG Eliseev, H. Li, A. Stintz, GT Liu, TC Newell, KJ Malloy, and LF Lester. Transition dipole moment of InAs/InGaAs quantum dots from experiments on ultralow-threshold laser diodes. *Applied Physics Letters*, 77:262, 2000. 3
- [46] TH Stievater, X. Li, DG Steel, D. Gammon, DS Katzer, D. Park, C. Piermarocchi, and LJ Sham. Rabi oscillations of excitons in single quantum dots. *Physical Review Letters*, 87(13):133603, 2001. 3
- [47] W.H. Press, S.A. Teukolsky, W.T. Vetterling, and B.P. Flannery. *Numerical recipes: the art of scientific computing*. Cambridge Univ Pr, 2007. 4

Acknowledgments We thank Mr. Christopher Ellis, Dr. Mikhail Erementchouk, and Dr. Volodymyr Turkowski for helpful discussions. We acknowledge computational support from the Institute for Simulation and Training STOKES HPCC and financial support from NSF (Grant No. ECCS-0725514), DARPA/MTO (Grant No. HR0011-08-1-0059), NSF (Grant No. ECCS-0901784), AFOSR (Grant No. FA9550-09-1-0450).

Competing Financial Interests The authors declare that they have no competing financial interests.